Technical Report: Supporting Internet-of-Things Analytics in a Fog Computing Platform

Hua-Jun Hong[1], Pei-Hsuan Tsai[1], An-Chieh Cheng[1], Md Yusuf Sarwar Uddin[2], Nalini Venkatasubramanian[2], and Cheng-Hsin Hsu[1]

[1]Department of Computer Science, National Tsing Hua University, Taiwan

[2]Department of Computer Science, University of California Irvine, CA

***Abstract*—Modern IoT analytics are computational and data intensive. Existing analytics are mostly hosted in cloud data centers, and may suffer from to high latency, network congestion, and privacy issues. In this paper, we design, implement, and evaluate a fog computing platform that runs analytics in a distributed way on multiple devices, including IoT devices, application gateways, and data-center servers. Several challenges need to be addressed to optimize the IoT analytics on our platform. In this paper, we focus on the core optimization problem: making deployment decisions to maximize the number of satisfied IoT analytics. We carefully formulate the deployment problem and design an efficient algorithm to solve it. Moreover, we conduct a detailed measurement study to derive the system models of the IoT analytics based on diverse QoS levels and heterogeneous devices to facilitate the optimal deployment decisions. We implement a testbed to conduct experiments, which show that the system models achieve reasonably good accuracy: as low as 5% (CPU) and 25% (RAM) deviations are observed. More importantly, 100% of the deployed IoT analytics satisfy the QoS requirements. We also conduct extensive simulations for larger scale scenarios. The simulation results reveal that our proposed algorithm outperforms a state-of-the-art algorithm by up to 89.4% and 168.3% in terms of number of satisfied IoT analytics and active devices. In addition, our proposed algorithm reduces 18.4%, 12.7%, and 898.3% of CPU, RAM, and network resource consumptions, respectively. Last, our proposed algorithm scales well and terminates in polynomial time.**

I. Introduction

Internet-of-Things (IoT) is getting more and more popular: the number of IoT devices worldwide is 22.9 billion in 2016, which is expected to reach 50.1 billion in 2020 [8]. Many modern IoT devices, such as Google Home [5] and Amazon Echo [1], enable IoT *analytics*, which collect, interpret, extract, and communicate hidden patterns from diverse sensor data. Because IoT analytics are computationally intensive, most existing IoT analytics run on cloud servers instead of IoT devices [34]. Doing so, however, has several drawbacks because IoT analytics are also data-intensive [3]. In particular, exchanging large amount of data over the best-effort Internet results in network congestion and long response time. On top of that, uploading sensitive data, such as videos captured at home, to cloud servers for analytics leads to privacy concerns [34].

To alleviate these limitations, we propose to: (i) perform some analytics operations on IoT devices, (ii) divide larger IoT analytics into several *operators*, which are the basic software components that can be deployed and run on IoT devices, and (iii) dynamically deploy operators on suitable IoT devices to maintain Quality-of-Service (QoS) targets, such as sampling rates of virtual sensors and response time of object recognizers. Therefore, organizing resources from many IoT devices into a *fog computing* platform becomes the enabler of implementing the above solution. Fog computing is proposed by Cisco [16] and generalized in several studies [21, 23, 33, 35], which concurrently leverages resources from cloud servers in data centers, application gateways in edge networks, and embedded IoT devices and laptop/desktop computers as end devices.

Fig. 1. Our envisioned ecosystem of fog computing platforms.

We collectively call these devices as *fog devices*, which are managed by a conceptually centralized server, as illustrated in Fig. 1. We envision a fog computing ecosystem with three parties. The *fog service provider* offers a platform to *application developers*, who write and sell IoT analytics (and other) applications. These IoT analytics are dynamically deployed in a distributed manner in, e.g., smart homes, smart cities, connected cars, and smart hospitals. *Fog users* are individuals who need IoT analytics, but do not have knowledge to develop them. Fog users, therefore, go to fog service providers and request to deploy specific IoT analytics at chosen QoS levels. Fog service providers then deploy the IoT analytics accordingly. This ecosystem is quite similar to existing mobile application stores and cloud computing platforms, but offers much higher flexibility, e.g., IoT analytics can now be done *outside* of data centers.

In this paper, we develop and optimize a fog computing platform to support IoT analytics. Several challenges need to be carefully addressed. First, matching resource requirements of operators with the available resources of fog devices is inherently computationally expensive. Moreover, the fog plat-

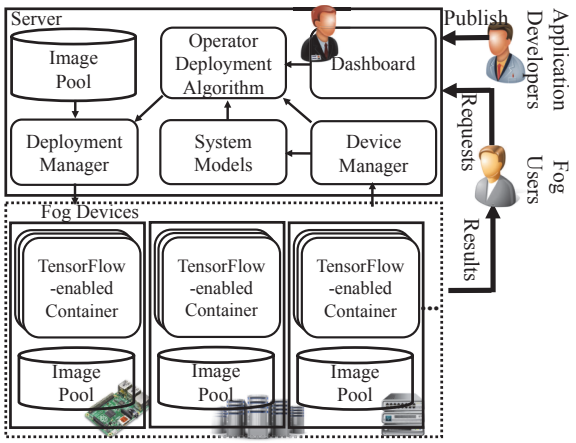

Fig. 2. The fog computing platform proposed for IoT analytics.

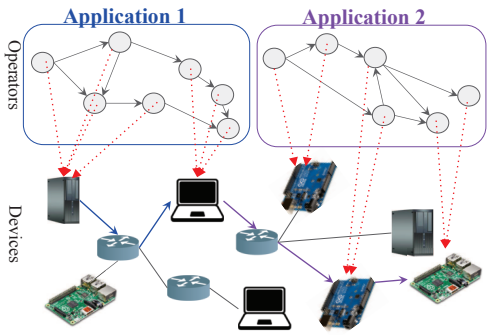

Fig. 3. The overview of our operator deployment problem.

form is shared by multiple IoT analytics with different target QoS levels, which also affect the resource requirements of operators. Intelligently deploying operators on fog devices to maximize the number of satisfied IoT analytics requests is the crux of optimizing the fog computing platform. The problem is referred to as the *operator deployment problem* throughout this paper. Second, fog devices are heterogeneous, and may not be powerful enough to run a complex analytics application. We adopt *graph processing* [31] as the programming model to help application developers build *multi-operator* IoT analytics. Third, several operators belong to different IoT analytics may be run on the same fog device. Provisioning resources of fog devices and rapidly deploying IoT analytics dictate *virtualization*.

We solve the three challenges in the following two steps.

- **An efficient operator deployment algorithm for IoT analytics** is developed to maximize the number of satisfied IoT analytics requests. The algorithm takes: (i) network bandwidth constraints, (ii) virtualization overhead, and (iii) required resource models into considerations. Our algorithm, tailored to address the first challenge, is more general than the ones in earlier work [17, 18, 19].
- **A real fog computing platform for IoT analytics** is constructed based on TensorFlow [13], Docker [4], and Kubernetes [9] to address the second and third challenges and to evaluate our algorithm. TensorFlow [13] supports graph processing and comes with analytics libraries. We adopt Kubernetes [9] to deploy, upgrade, monitor, and migrate operators in virtualized Docker [4].

Our experiment and simulations evaluations are both very promising. For example, in simulations, our proposed algorithm outperforms a state-of-the-art algorithm [18] by up to (i) 89.4%, (ii) 168.3%, and (iii) 898.3% in terms of the number of satisfied requests, the number of active fog devices, and the consumed network resources, respectively.

II. System Overview

Fig. 2 gives an overview on our fog computing platform, which consists of the following six major components.

- **System models.** The system models are derived through real experiments. The models predict the expected resource consumptions (e.g., CPU or network) under different QoS levels (e.g., report frequency and recognition accuracy) and different specifications of fog devices.
- **TensorFlow-enabled container.** We include TensorFlow [13] and its analytics libraries in Docker container [4]. Containers are light-weight virtual machines suitable to IoT analytics, because of their smaller footprints and shorter initialization time.
- **Device manager.** We extend Kubernetes to collect more device status, including: (i) the resource utilizations, e.g., CPU and RAM usage, (ii) the device locations, e.g., GPS readings, and (iii) sensor availability and capability, e.g., existence of depth cameras at VGA resolution.
- **Deployment manager.** We build a deployment manager on Kubernetes to remotely launch specific Docker image on a chosen fog device. The deployment manager also supports other management tasks, such as killing, restarting, and migrating containers.
- **Image pool.** We package each operator of IoT analytics into a Docker image. These images are first stored in the image pool at the server, and then are transferred to and cached at the image pools of the chosen fog devices.
- **Operator deployment algorithm.** The algorithm solves the core research problem of this paper. It makes decisions to deploy which operators on which fog deices for individual IoT analytics requests. The requests come with diverse QoS targets and deployed locations. The goal of the algorithm is to maximize the number of satisfied requests, while considering: (i) the expected resource consumptions, (ii) the spatial requirements of requests, (iii) the required sensors, and (iv) the available resources of fog devices. A request is satisfied iff the target QoS is achieved at the specified location. Fig. 3 summarizes our operator deployment problem. Each operator graph represents a multi-operator analytics, and the device graph abstracts away the fog devices and network infrastructure.

III. Operator Deployment Problem: Formulation and Algorithm

The operator deployment problem is formulated and solved in this section.

A. Notations

Table I summarizes the symbols used in this paper. Let $\mathbf{A}$ be a set of IoT analytics, $\mathbf{Q}$ be a set of requests, $\mathscr{A}_q$ be the IoT analytic of request q, and s_q be the QoS target of request q, for any $q \in \mathbf{Q}$. We let $\hat{G}_a = <\hat{\mathbf{V}}_a, \hat{\mathbf{E}}_a>$ be the operator graph of IoT analytic a, for all $a \in \mathbf{A}$, where $\hat{\mathbf{V}}_a$ is is the operator set and $\hat{\mathbf{E}}_a$ is the edge set. $\dot{F}(\cdot)$ and $\bar{F}(\cdot)$ denote the system models, which capture the required resources of each operator and edge, respectively. We concertize the system models in our testbed in Sec. IV. Moreover, we use $J_{q,i,i'}$ to represent the parent and children relationship between any two operators. More specifically, $J_{q,i,i'} = 1$ means operator i is the parent operator of i'. We let $G = <\mathbf{V}, \mathbf{E}>$ be the device graph, where $\mathbf{V}$ is a set of the fog devices and $\mathbf{E}$ is a set of the links. Each device k has its resource capacity $R_{k,u}$ of resource type u, where $k \in \mathbf{V}$ and $u \in \mathbf{U}$. Each physical link (k, k') has its capacity $B_{(k,k')}$. We use $T_{(k,k'),l}$ to describe whether link l is on the path from device k to device k'. Last, the operators have sensor and location requirements from the corresponding requests. We let $\mathbf{V}_{q,i}$ as an available device set that satisfies the sensor and location requirements of operator i in request q. The path between two fog devices can be computed by various routing algorithms, and the shortest paths are adopted if not otherwise specified.

TABLE I
Symbols Used Throughout this Paper

Sym.	Description
$\mathbf{A}$	Set of all IoT analytics
$\mathbf{Q}$	Set of all requests
$\mathscr{A}_q$	IoT analytic of request q
s_q	QoS target of request q
$\mathbf{U}$	Set of considered resource types, such {CPU, RAM, ...}
$\hat{G}_a$	Operator graph $<\hat{\mathbf{V}}_a, \hat{\mathbf{E}}_a>$ of IoT analytic a
G	Device graph $<\mathbf{V}, \mathbf{E}>$
$\hat{\mathbf{V}}_a$	Set of operators in $\hat{G}_a$
$\hat{\mathbf{E}}_a$	Set of edges in $\hat{G}_a$
$\mathbf{V}$	Set of fog devices in G
$\mathbf{E}$	Set of links in G
$\mathbf{V}_{q,i}$	Set of fog devices that can host operator i of request q
$R_{k,u}$	Capacity of resource u of device k
B_l	Capacity of link l
$T_{(k,k'),l}$	Indicator of link l in on path from device k to k'
$J_{q,i,i'}$	Indicator of operator i is parent of operator i'

B. Problem Formulation

Lemma 1 (Hardness)**.** *The operator deployment problem is NP-hard.*

Proof. (Sketch) The operator deployment problem can be reduced from an NP-hard Multiple Knapsack Problem (MKP). The MKP problem puts as many objects as possible into multiple knapsacks with diverse capacities. If we let $|\hat{\mathbf{V}}_A| = 1$ and $B_l =$ unlimited, we can map knapsacks as fog devices and objects as requests without any network constraint. In this way, we reduce the MKP problem to our operator deployment problem in polynomial time. This yields the hardness proof. □

Since the operator deployment problem is NP-hard, we formulate the problem as an ILP (Integer Linear Programming) problem:

$$\max \sum_{q \in \mathbf{Q}} p_q \tag{1a}$$

$$st: z_q = \sum_{i \in \hat{\mathbf{V}}_{\mathscr{A}_\mathbf{q}}} \sum_{k \in \mathbf{V}_{q,i}} x_{q,i,k} / |\hat{\mathbf{V}}_{\mathscr{A}_\mathbf{q}}| \ \forall q \in \mathbf{Q}; \tag{1b}$$

$$z_q - 1 < p_q \leq z_q \ \forall q \in \mathbf{Q}; \tag{1c}$$

$$\sum_{k \in \mathbf{V}_{q,i}} x_{q,i,k} \leq 1 \ \forall q \in \mathbf{Q}, i \in \hat{\mathbf{V}}_{\mathscr{A}_\mathbf{q}}; \tag{1d}$$

$$\sum q \in \mathbf{Q} \sum_{i \in \hat{\mathbf{V}}_{\mathscr{A}_q}} \dot{F}(\cdot) x_{q,i,k} \leq R_{k,u} \quad \forall k \in \mathbf{V}_i, u \in \mathbf{U}; \tag{1e}$$

$$\sum_{q \in \mathbf{Q}} \sum_{i \in \hat{\mathbf{V}}_{\mathscr{A}_q}} \sum_{i' \in \hat{\mathbf{V}}_{\mathscr{A}_q}} \sum_{k \in \mathbf{V}_{q,i}} \sum_{k' \in \mathbf{V}_{q,i'}} y_{q,(i,i'),(k,k')} J_{q,i,i'} T_{(k,k'),l} \bar{F}(\cdot) \leq B_l \ \forall l \in \mathbf{E}; \tag{1f}$$

$$x_{q,i,k} = \sum_{k' \in \mathbf{V}_{q,i'}} y_{q,(i,i'),(k,k')} \quad \forall q \in \mathbf{Q}, i \in \hat{\mathbf{V}}_{\mathscr{A}_q}, i' \in \hat{\mathbf{V}}_{\mathscr{A}_q}, k \in \mathbf{V}_{q,i}; \tag{1g}$$

$$x_{q,i',k'} = \sum_{k \in \mathbf{V}_{q,i}} y_{q,(i,i'),(k,k')} \quad \forall q \in \mathbf{Q}, i \in \hat{\mathbf{V}}_{\mathscr{A}_q}, i' \in \hat{\mathbf{V}}_{\mathscr{A}_q} k' \in \mathbf{V}_{q,i}; \tag{1h}$$

$$p_q, x_{q,i,k} \in \{0,1\} \ \forall q \in \mathbf{Q}, i \in \hat{\mathbf{V}}_{\mathscr{A}_\mathbf{q}}, k \in \mathbf{V}_{q,i}. \tag{1i}$$

In this formulation, $x_{q,i,k}$ is the decision variable, where $x_{q,i,k} = 1$ iff operator i of request q is deployed on device k. The objective function in Eq. (1a) counts the number of satisfied requests, where an intermediate variable $p_q = 1$ iff request q is satisfied. Eqs. (1b) and (1c) make sure that when request q is satisfied, all the operators of request q are deployed. Eq. (1d) makes sure that each operator is deployed once. Eq. (1e) ensures that the required resources of the deployed operators do not exceed the resource capacities of the devices. Eq. (1f) makes sure that the required bandwidth of the deployed containers does not exceed the capacity of the network links. Eqs. (1g) and (1h) define another intermediate variable $y_{q,(i,i'),(k,k')}$, which is 1 iff edge (i, i') of request q is mapped to physical path (k, k'). The intermediate variables $y_{q,(i,i'),(k,k')}$ are used to embed the operator graphs in the device graph.

C. Proposed Algorithm and Analysis

Because our problem is NP-hard, we propose a greedy operator deployment algorithm based on three intuitions (steps):

- **Scarcest resource first.** Because requests demand for different resource types at the same time, the scarcest

resource becomes the limiting factor. To satisfy as many requests as possible, we identify the scarcest resource (after normalization), sort requests in the ascending order on the scarcest resource, and then consider the requests consuming less scarcest resource earlier. The result of this step is a sorted set of undeployed requests.

- **Shortest path first.** For each request, we consider all pairs of feasible fog devices for the source and destination operators. Because shorter paths generally lead to lower overall network loads and shorter end-to-end delays, we select the pair of fog devices with the shortest path for the source and destination operators. The result of this step is the deployment decisions of the source and destination operators.
- **Early feature extraction.** Upon the source and destination operators are deployed, we start to deploy the remaining operators. Since the operators in typical IoT analytics extract increasingly higher-level features that are generally more compact, deploying the operators closer to the parent operator reduces the network workload and the transfer time. We employ a system parameter H and only consider deploying a child operator on fog devices within H hops from its parent operator. H is typically a small constant, which also allows us to reduce our time complexity. The result of this step is the deployment decisions of operators other than the source and destination ones.

We refer to this algorithm as *SSE* algorithm, which are the initials of the three intuitions. Fig. 4 gives the pseudocode of our algorithm. Lines 1–2 implement the first intuition, sort the requests in $\mathbf{Q}$ by the scarcest resource type. Lines 4–13 realize the second intuition, where we store source and destination pair of devices into $\mathbf{M}$ and sort them by their path lengths. Lines 14–19 implement the third intuition to consider the fog devices that are closer to source device first. Lines 20–21 check the constraints and make the final deployment decisions.

Lemma 2 (Correctness and Time Complexity)**.** *Our algorithm gives a feasible solution in polynomial time.*

Proof. The correctness is ensured by lines 20–21. For complexity, we first sort the requests $\mathbf{Q}$ by the scarcest resource type in lines 1–2, which has a complexity of $O(|\mathbf{Q}|\log|\mathbf{Q}|)$. The for-loop starting from lines 3 to line 19 goes through all the requests. For each request q, we go through all possible pairs of devices sorted by the number of hops for deploying the source and destination operators in lines 4–6. We then create $\mathbf{W}$ to store and go through all the operators $i' \in \mathbf{W}$ until $\mathbf{W}$ is empty in line 9–11. In lines 13–22, We create $\mathbf{D}_h$ to store fog devices and $\mathbf{N}'_i$ to store child operators of i'. We then sort $\mathbf{D}_h$ by the number of hops to destination device; go through the sorted devices and child operators to deploy the operators without violating Eqs. (1d) to (1f). We let $K = |\mathbf{V}|$, $I = max_{a\in\mathbf{A}}(|\hat{\mathbf{V}}_\mathbf{a}|)$, and $P = |\mathbf{Q}|$. The complexity of lines 3–19 is $O(P(K^2\log K^2 + K^2 I(K\log K + HIK)))$, which dominates the complexity of our algorithm and is polynomial. We notice that I (the maximal number of operators in each request) and H (the hop limit) are typically bounded integers. Under this assumption, the time complexity can be written as $O(PK^3\log K + PK^2\log K^2)$. □

Inputs: Request info, such as QoS target s_q, analytics info, such as operator graphs $\hat{G}_a$, device info, such as device resource capacity $R_{k,u}$, and link capacity B_l.
Output: The deployment decision $x_{q,i,k}$.

1: **let** $\hat{C}_q$ be the scarcest resource u' required by q
2: **sort** $\mathbf{Q}$ by $\hat{C}_q$ in asc. order
3: **for** $q \in \mathbf{Q}$ **do**
4: **let** $\mathbf{M}$ to store pairs of devices, including source device $\hat{k}$ and destination device $\check{k}$, which are feasible to launch source $\hat{i}$ and destination operators $\check{i}$ of request q, respectively
5: **sort** $\mathbf{M}$ on the shortest path length from $\hat{k}$ to $\check{k}$ in asc. order
6: **for** $(\hat{k}, \check{k}) \in \mathbf{M}$ **do**
7: **let** $x_{q,\hat{i},\hat{k}} = 1$
8: **let** $x_{q,\check{i},\check{k}} = 1$
9: **let** $\mathbf{W}$ be all the deployed operators
10: **add** $\hat{i}$ and $\check{i}$ to $\mathbf{W}$
11: **while** $\mathbf{W}$ is not empty **do**
12: **pop** an operator i' from $\mathbf{W}$
13: **let** $\mathbf{N}'_i$ be the child operators of i'
14: **let** H be hop limit
15: **let** $\mathbf{D}_h$ be devices that are h hops to the device running operator i'
16: **sort** $\mathbf{D}_h$ on the number of hops to $\check{k}$
17: **for** $h = 0, 1, 2, \ldots, H$ **do**
18: **for** $i \in \mathbf{N}_{i'}$ **do**
19: **for** $k \in \mathbf{D}_h$ **do**
20: **if** Eqs. (1d) to (1f) are satisfied **then**
21: **let** $x_{q,i,k} = 1$
22: **add** i to $\mathbf{W}$
23: **if** operators of request q are not all deployed **then**
24: **clear** all deployed operator of request q

Fig. 4. The pseudocode of our proposed SSE algorithm.

IV. Testbed and Experiments

In this section, we realize a testbed of our fog computing platform for: (i) conducting a measurement study to derive our system models and (ii) evaluating the derived models and the performance of our fog computing platform.

A. Testbed Implementations

Fig. 5 illustrates our testbed, which consists of: (i) an Intel i5 workstation running Ubuntu, Docker [4], and Kubernetes [9] as the server and (ii) 5 Intel PCs (1.8 GHz 8-core i7 CPUs) and 5 Raspberry Pi 3 (1.2 GHz 4-core ARM CPUs) as the fog devices running Ubuntu and HypriotOS, respectively. We implement the software components presented in Fig. 2 on the server and fog devices. The server and devices are connected with an Ethernet switch in a private network. To emulate WiFi-based IoT networks, we adopt a traffic shaper [14] to throttle the bandwidth at 8 Mbps [20]. To avoid overloading the fog devices, we reserve 20% of resources for operations other than IoT analytics, e.g., OS scheduling and resource monitoring.

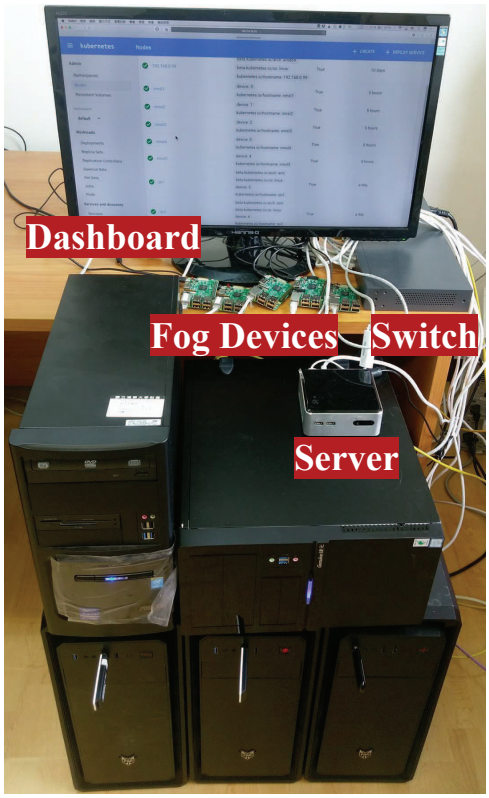

Fig. 5. Testbed of our fog computing platform.

We implement the multi-operator IoT analytics using TensorFlow [13], in which every application is represented as a graph consisting of *nodes* and *links*. The nodes can be simple tasks, such as additions and subtractions, or very complex machine learning tasks. The links are the data flows among nodes. We use TensorFlow *tags* to split every graph into multiple smaller subgraphs, where each subgraph contains one or multiple nodes and associated links. These subgraphs are essentially the *operators* in our fog computing platform, which are the units of deployments.

However, IoT analytics may require some features that are not available in TensorFlow. For example, OpenCV [12] is needed for processing images and librosa [10] is needed for analyzing audios. These additional libraries are quite large and take hours to be compiled. Therefore, installing these libraries on-the-fly is infeasible. On the other hand, reimplementing the features in TensorFlow incurs high engineering overhead, which may not be worth it. Fortunately, our fog computing platform achieves short deployment time using Docker images. Furthermore, TensorFlow does not natively support stream processing, and we add a queue between any two adjacent operators to increase the overall performance.

We develop three sample multi-operator IoT analytics: (i) air pollution monitor, (ii) sound classifier, and (iii) object recognizer to show the practicality of our platform. Each of them contains a large number of nodes, e.g., the object recognizer has 348 nodes. We split each TensorFlow graph into a few operators (subgraphs) as follows.

- **The air quality monitor** receives four gas sensor readings in JSON format through the MQTT protocol [11]. It then parses the JSON objects and calculates the moving averages of individual gas sensors. The results can be used to detect emergency events, such as explosive gas leaking. We split the IoT analytic into 5 operators. The first operator subscribes all gas sensor data via MQTT. The other four operators are responsible for calculating the moving averages of the four gas sensors, respectively.
- **The sound classifier** detects different types of sounds for community safety. For example, this IoT analytic may detect a gun shot and automatically notify the police. It adopts a pre-trained four-layer neural network for analyzing the audio inputs. The IoT analytic is split into 5 linear operators. The first operator gathers the audio data, while the other four operators execute the four layers of the neural network, respectively.
- **The object recognizer** collects and analyzes camera images for recognizing objects in them. It employs a pre-trained neural network with more than 10 layers. We split the IoT analytic into 3 operators for input, hidden, and output layers, respectively. The first operator also captures and resizes the camera images using OpenCV [12].

Figs. 87**??** show a sample TensorFlow graph of our sound classifier, recognized result of our object recognizer, and web interface of our air quality monitor.

B. System Model Derivation

The system models map the target QoS levels of different IoT analytics to the required resources on heterogeneous hardware specifications, as illustrated in Fig. 9. The parameters of operator model $\dot{F}(\mathscr{A}_q, s_q, i, u, k)$ and edge model $\bar{F}(\mathscr{A}_q, s_q, (i, i'))$ are derived in the following. First, we conduct an offline measurement study to derive the system model of Raspberry Pis (the lowest-end devices). For Intel PCs (more powerful devices without existing models), we use the models of less powerful devices for *bootstrapping*. We then update the system models online to derive the customized system models. Using system models of less powerful devices for bootstrapping prevents us from overloading the fog devices. Although we only have two types of fog devices in the testbed, the same procedure is applicable to more heterogeneous devices.

We model the following three resources:

- **CPU load:** the physical CPU load in percentage reported by Docker stats API.
- **RAM usage:** the total physical memory usage reported by Docker stats API.
- **Network throughput:** total traffic amount (in both directions) reported by Tcpdump.

We adopt different invocation frequencies as the QoS parameters; other QoS parameters may also be adopted if needed. Particularly, in our experiments, we choose the following sample parameters: (i) $\{0.25, 0.5, 1, 2, 4\}$ Hz in the air quality monitor, (ii) $\{6/60, 7/60, 8/60, 9/60, 10/60\}$ Hz in the object

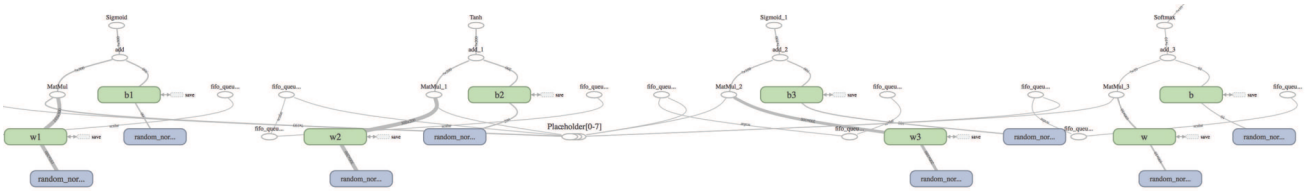

Fig. 6. A sample TensorFlow graph of our sound classifier.

Fig. 7. A sample result of our object recognizer.

Fig. 8. A sample web interface of our air quality monitor.

recognizer, and (iii) $\{5/60, 6/60, 7/60, 8/60, 9/60\}$ Hz in the sound classifier. Each QoS level of every IoT analytic is executed 5 times with 60-sec durations. We report the average, after filtering out the results that deviate from the average for more than 1.7 times of the standard deviation.

Fig. 10 shows the system models of a sample operator (CPU and RAM) and a sample edge (network) in the object recognizer. We make a few observations on the sample results

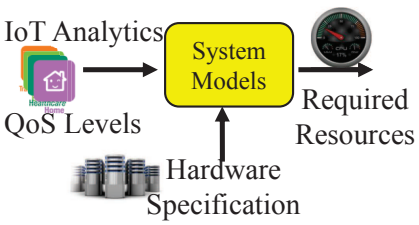

Fig. 9. Our proposed system models.

TABLE II
THE MEAN (STANDARD DEVIATION) R-SQUARE VALUES AND P-VALUES AMONG ALL OPERATORS AND EDGES.

IoT Analytics	CPU Load		Network Throughput	
	R-Square	P-Value	R-Square	P-Value
Air Quality Monitor	0.99 (0.000023)	<0.001	0.99 (0.000001)	<0.001
Sound Classifier	0.85 (0.023263)	<0.010	0.84 (0.069494)	<0.010
Object Recognizer	0.99 (0.012540)	<0.010	0.97 (0.004982)	<0.010

and adopt the following regression models. First, we find that the RAM usage (Fig. 10(b)) remains the same under different QoS parameters. Therefore, we model it as a constant value, which gives us an average error of 0.4% and a maximum error of 1%. For the CPU load (Fig. 10(a)) and network throughput (Fig. 10(c)), we adopt power models, which give 0.99 R-square scores in both cases. The operator and edge models are given below:

$$\dot{F}(\mathscr{A}_q, s_q, i, u, k) = \begin{cases} d_{\mathscr{A}_q, s_q, i, k} & u = \text{RAM} \\ \dot{a}_{\mathscr{A}_q, i, k} s_q^{\dot{b}_{\mathscr{A}_q, i, k}} + \dot{c}_{\mathscr{A}_q, i, k} & u = \text{CPU} \end{cases}$$

$$\bar{F}(\mathscr{A}_q, s_q, (i, i')) = \bar{a}_{\mathscr{A}_q, (i, i')} s_q^{\bar{b}_{\mathscr{A}_q, (i, i')}} + \bar{c}_{\mathscr{A}_q, (i, i')}$$

Similar observations can be made on other operators and edges. We report the mean R-square scores of the CPU and network models with their standard deviations in Table II. This table shows that our system models are fairly accurate. Moreover, the same table also reports p-values (< 0.01), which indicates that the regression is statistically significant.

C. Validation

We run the following experiment for 15 iterations, where the offline system models are initially used for both Raspberry Pis and Intel PCs to drive our operator deployment algorithm. Based on the actual resource consumption, we update our system models after each iteration that lasts for about 3 minutes. In each iteration, we randomly generate requests of three sample IoT analytics with 0.1 to 4 Hz random QoS levels. We up-sample the QoS levels by 10% as a small buffer for workload surges. Specifically, we generate a large number of requests, and execute our operator deployment algorithm to deploy as many requests as possible. Although network conditions affect the download time of Docker images, disseminating Docker images efficiently is out of the scope of this work. Therefore, we assume all the Docker images are already cached in the image pools of fog devices. Sample experiment results are given below.

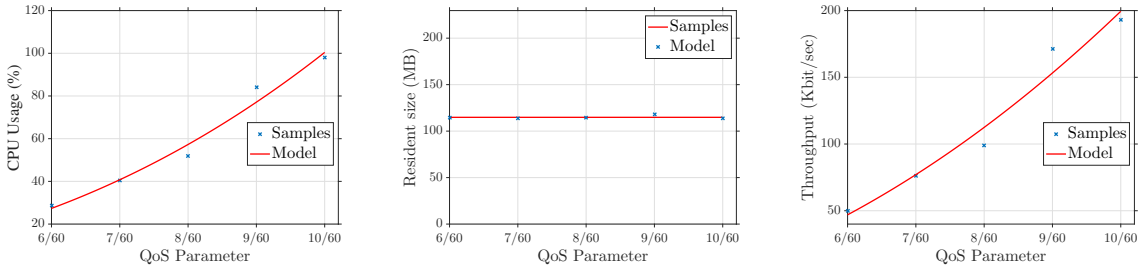

(a) (b) (c)

Fig. 10. The system models of (a) CPU load, (b) RAM usage, and (c) network throughput. Sample results from the object recognizer.

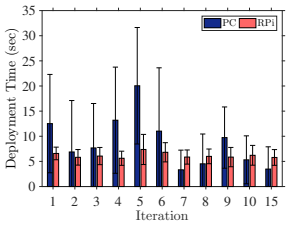

Fig. 11. The average deployment time of operators in each iteration.

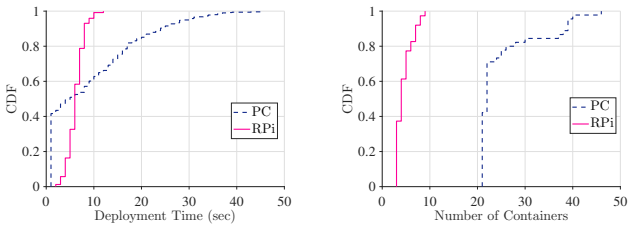

(a) (b)

Fig. 12. (a) Most operators deployed on Intel PCs take less time than on Raspberry Pis and (b) the number of containers created on Intel PCs are far more than on Raspberry Pis.

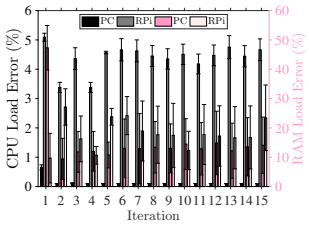

Fig. 13. Online updates of our system models are effective.

TABLE III
QoS Satisfaction Rate and Number of Rejected Requests over Iterations

	Iter. 1		Iter. 2		Iter. 3		Iter. 4		Iter. 5	
Received Requests	**Rejected Requests**	**QoS Satis. Rate**	**Rejected Requests**	**QoS Satis. Rate**	**Rejected Requests**	**QoS Satis. Rate**	**Rejected Requests**	**QoS Satis. Rate**	**Rejected Requests**	**QoS Satis. Rate**
4	0	100%	0	100%	0	100%	0	100%	0	100%
8	0	100%	0	100%	0	100%	0	100%	0	100%
16	0	79%	0	100%	0	100%	0	100%	0	100%
32	0	89%	10	95%	10	100%	10	100%	10	100%
64	22	71%	42	95%	42	95%	42	100%	42	100%

Operators are deployed almost instantly in our platform. Fig. 11 reports the average deployment time of operators in each iteration. The figure reveals that the operators take less than 20 seconds on average to be deployed, which is sufficient for most IoT analytics. As Fig. 12(a) shows, over 50% of operators deployed on Intel PCs take less time than on Raspberry Pis because Intel PCs have stronger compute power. The rest of deployments take more time on Intel PCs than on Raspberry Pis because there are considerably more operators running on PC than Raspberry Pis, as reported in Fig. 12(b). When a large number of containers are simultaneously created on the same device, the I/O overhead is significantly increased.

Our system models are reasonably accurate and support heterogeneous fog devices. We report the system model error rates of two sample models: (i) power models of CPU loads and (ii) constant models of RAM usage in Fig. 13. This figure shows that our system models become increasingly accurate over iterations and are stable after 5 iterations. More specifically, the CPU load errors are less then 5% and the RAM usage errors are less then 25% on average after 5 iterations.

Our operator deployment algorithm satisfies most of the requested QoS levels. Table III shows the *QoS satisfaction rate* and *number of rejected requests* under different numbers of requests received from fog users. The QoS satisfaction rate is the fraction of deployed requests that meet the QoS target, and the rejected requests are not deployed by our algorithm due to lack resources. The table leads to three observations: (i) the QoS satisfaction rate is getting higher over iterations. At the fifth iteration, the QoS satisfaction rate reaches to 100%, (ii) more received requests require more iterations to satisfy all the requests, and (iii) once our platform is fully loaded, some requests are rejected to maintain the QoS levels of deployed requests.

The above experiments demonstrate the practicality and efficiency of our models, algorithm, and platform. For larger scale evaluations, we perform detailed simulations in the next section.

V. Simulations

In this section, we conduct simulations to exercise a wider spectrum of system parameters in a larger fog computing platform.

A. Setup

We build a detailed simulator in Python. In this simulator, we implement our SSE and three baseline algorithms, which are Random, Linear, and Optimal Data Stream Processing Placement (ODP) [18]. The Random algorithm mimics a fog computing platform without a central controller, and deploys operators on random devices. The Linear algorithm greedily deploys operators from the source fog devices to adjacent devices, while taking the resource, sensor, and location constraints into considerations. The ODP algorithm is a state-of-the-art operator deployment algorithm with a flexible objective function. We adapt its objective function to maximize the number of satisfied requests for fair comparisons. The ODP algorithm employs a commercial ILP solver: CPLEX [7], which may take prohibitively long time to terminate. Therefore, it was recommend to set a 500-sec cap on the execution time [18]. We run each simulation five times with the four algorithms for comparisons. The algorithms make deployment decisions of Q requests, which are received by our fog computing platform in every batch time of T.

BRITE [2] is used to generate the network topology among the fog devices and the server. The device coordinates generated by BRITE are fit to the geographical area of Taipei city, Taiwan. Each fog device has a random CPU capacity between 100% and 800% (corresponding to number of cores) and a random RAM capacity between 1 and 16 GB. Each fog device comes with a random wireless network interface with the following link capacity: 45 kbps with LoRa [26], 8 Mbps with WiFi [20], and 25 Mbps with 4G [6]. Poisson processes with 1-min average arrival time and 10-min average departure time are used for generating requests. In this way, the number of active requests steadily increases over time. Each request randomly picks one of the three IoT analytics with random QoS targets between 0.1 and 4 Hz. The system models (of PCs and Raspberry Pis) derived in our earlier experiments are used in the simulations. Each request randomly occurs in one of the 12 districts of Taipei city. We consider random sensors, including cameras, microphones, (4 types of) gas sensors, and 4G cellular dongles. IoT analytics are associated with the corresponding sensors. Moreover, the destination operators always require the 4G dongles, in order to distribute results to citizens.

We consider the following performance metrics.

- **Number of deployed requests.**
- **Number of satisfied requests,** which comply with the constraints in Eqs. (1d) and (1f).
- **Number of overloaded links.**
- **Number of active devices,** which host one or more operators.
- **Resource loads**, which are device CPU, RAM, and network usages.
- **Running time** of the operator deployment algorithms.

We run 48-hour simulations on an AMD 64-core workstation. We consider the number of fog devices $|\mathbf{V}| \in \{10, 25, 50, 75, 100\}$ and the maximal number of hop $H \in \{1, 5, 10, 15, 20\}$. We let $|\mathbf{V}| = 100$ and $H = 10$ if not otherwise specified. We repeat each simulation 5 times and report average results with 95% confidence intervals if applicable.

B. Results

Our proposed SSE algorithm results in QoS improvements. Fig. 14 reports the overall QoS achieved by different algorithms. Fig. 14(a) shows that Random and ODP deploy up to 11.53 times and 18.9% more requests compared to our SSE algorithm; in contrast, our SSE algorithm deploys up to 1.7 times more requests than Linear. In Fig. 14(b), we observe that our SSE algorithm satisfies up to 171% and 89.4% more requests than Linear and ODP, respectively. On the other hand, Random satisfies zero request after running for 14 hours. The inferior performance of Random and ODP is because they do not capture the detailed resource constraints, and thus are too aggressive and overload the fog computing platform. In contrast, Linear algorithm limits its operator deployment decisions to adjacent devices, and thus is too conservative. To demonstrate this, we plot the number of overloaded links in Fig. 14(c), where Random and ODP result in as many as 13 and 21 overloaded links, while Linear (and our SSE algorithm) leads to none. Since Random and Linear suffer from significantly few number of satisfied requests, we no longer consider them in the rest of this paper.

Our proposed SSE algorithm reduces energy cost and carbon footprint. Fig. 15 reports the number of the active devices over time. It shows that our SSE algorithm turns off up to 168.3% more devices, compared to ODP yet satisfying more requests as shown in Fig. 14(b). Putting more (inactive) fog devices into asleep reduces the energy cost and carbon footprint.

Our proposed SSE algorithm is resource efficient. Fig. 16 shows the peak overall and distributions of resource consumption. In particular, Fig. 16(a) reports the peak total resource consumption, which shows that our SSE algorithm reduces 18.4%, 12.7%, and 898.3% resource consumptions in terms of CPU, RAM, and network. Figs. 16(b)–16(d) plot CDF of the resource consumption from individual fog devices. These figures clearly reveal that our SSE algorithm results in much better resource efficiency, as it consumes less resources and satisfies more requests.

Our proposed SSE algorithm is scalable. Table IV reports the maximal running time of the operator deployment algorithms throughout 48-hour simulations under different number of fog devices. This table shows that the running time of ODP exceeds its 500-sec threshold with merely 100+ fog devices. Moreover, ODP's running time grows exponentially. In contrast, our SSE algorithm only takes 12.22 sec to make the deployment decisions with 100 fog devices, and its running grows linearly.

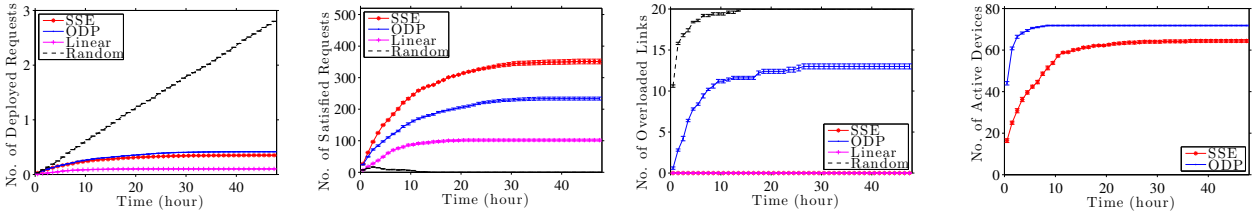

(a) (b) (c)

Fig. 14. QoS improvement of our SSE algorithm, in: (a) the number of deployed requests, (b) the number of satisfied requests, and (c) the number of overloaded links.

Fig. 15. The number of active fog devices.

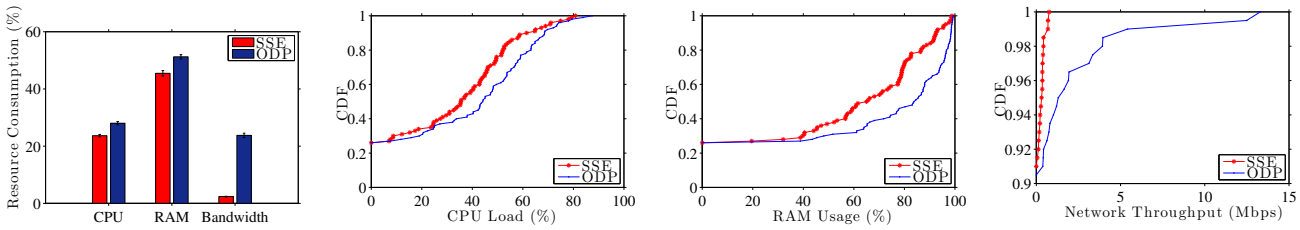

(a) (b) (c) (d)

Fig. 16. Resource efficiency improvement of our SSE algorithm: (a) peak overall resource consumption, (b) CPU load, (c) RAM usage, and (d) network throughput distributions of fog devices.

TABLE IV
MAXIMAL RUNNING TIME (SEC) OF OPERATOR DEPLOYMENT ALGORITHMS

No. Devices	10	25	50	75	100
SSE	0.41	1.25	6.11	10.27	12.22
ODP	3.87	24.66	195.93	300.83	>500

VI. Related Work

Fog computing. Fog computing is proposed by Cisco [16], and has been used in IoT platforms. For example, Wu et al. [35] leverage drones as fog devices to collect, process, and disseminate IoT data. Giang et al. [21] present a distributed programming model for IoT applications in fog computing platforms. Chun et al. [33] propose a pub/sub-based fog computing platform for connected cars. However, these studies do not dynamically deploy IoT applications to the heterogeneous fog devices.

Several studies [15, 27, 28, 30] apply virtualization technologies on fog computing platforms for dynamic and transparent deployment, remote management, and application isolation. However, they do not rigorously solve the operator deployment problem. Saurez et al. [32] propose to split applications for distributed deployment, but the deployment decisions are predefined by application developers, e.g., a machine learning operator is *always* run in data centers. In contrast, our proposed platform is much more flexible when deploying operators.

Graph processing. The input of Pregel [25] is an application represented as a graph with vertices and edges. The vertices are operators, which communicate among one another via a message passing mechanism. Khayyat et al. [24] extend Pregel for dynamic graph partitioning, which divides each graph into several subgraphs. The graph partitioning problem is essentially the same as the operator deployment problem in the literature of *streaming processing* [22]. Salihoglu et al. [31] enhance Pregel to reduce the communication traffic. These studies [22, 24, 25, 31] focus more on library design without considering IoT analytics and virtualization, nor do they solve the operator deployment problem.

The operator deployment problem has been solved under rather strong assumptions, e.g., Eidenbenz and Locher [19] propose a tree-based approximation algorithm for well-connected servers in data centers, which is not applicable to IoT analytics. In the literature, similar problem has also been solved in more distributed environments. For example, Pietzuch et al. [29] adapt to dynamic environments, such as network latency and data rates, to compute the deployment decisions of operators. They propose an algorithm based on the overhead of communicating among devices to solve the problem. Cardellini et al. [17, 18] consider the constraints on both devices and networks. They formulate an ILP (Integer Linear Programming) problem and optimally solve it with a commercial solver, which may be time consuming. Compared to our work, these studies [17, 18, 29] don't conduct detailed measurements nor model resource consumption and virtualization overhead. Furthermore, the operators considered in their papers are much more primitive, compared to the ones used in IoT analytics.

VII. Conclusion

In this paper, we study the operator deployment problem to maximize the number of satisfied IoT analytics requests with diverse target QoS levels in a fog computing platform. This

platform features: (i) graph processing as the programming model, (ii) lightweight virtualization for resource provisioning, and (iii) a novel operator deployment algorithm for deployment decisions. Our algorithm carefully captures the resource constraints, such as CPU, RAM, and bandwidth, which are modeled by our proposed system models. We design, develop, and implement a testbed to quantify: (i) the error rates of our system models, which are as low as 5% (CPU) and 25% (RAM), (ii) QoS satisfaction rate, which reaches 100% after at most 5 iterations, and (iii) operator deployment time, which is less than 20 secs on average. For larger scale evaluations, we conduct extensive simulations using traces collected from the testbed. The simulation results show that Random and Linear algorithms suffer from unacceptable number of satisfied requests. Moreover, our algorithm outperforms the state-of-the-art ODP algorithm by up to 89.4%, 168.3%, and 898.3% in terms of the number of the satisfied requests, the number of active fog devices, and the consumed network bandwidth, respectively. Last, our algorithm runs fast (12 secs for 100 fog devices) and scales well (linear growth rate).

This paper focus on IoT analytics running on fog computing platform, which integrates resources from end devices to data centers. Even we solve many critical challenges in this paper, many open issues still need to be addressed: (i) estimating the available resources of fog devices, such as personal computers that do not fully-controlled by the fog service provider, (ii) making migrating decisions to adapt to high resource dynamicity, such as network dynamicity to guarantee QoS, and (iii) requiring a mechanism to reserve network resources for the IoT analytics. We believe that the experiences learned from this paper sheds some lights on the future researches.

REFERENCES

[1] Amazon echo. https://www.amazon.com/Amazon-Echo-Bluetooth-Speaker-with-WiFi-Alexa/dp/B00X4WHP5E.

[2] BRITE. https://www.cs.bu.edu/brite/.

[3] Digital Universe Invaded by Sensors. https://www.emc.com/about/news/press/2014/20140409-01.htm.

[4] Docker. https://www.docker.com.

[5] Google home. https://madeby.google.com/home/.

[6] How fast is 4G? http://www.4g.co.uk/how-fast-is-4g/.

[7] IBM CPLEX optimizer. http://www-01.ibm.com/software/commerce/optimization/cplex-optimizer/.

[8] Internet of Things (IoT): number of connected devices worldwide from 2012 to 2020 (in billions). https://www.statista.com/statistics/471264/iot-number-of-connected-devices-worldwide/.

[9] Kubernetes. http://kubernetes.io/.

[10] librosa. https://github.com/librosa/librosa.

[11] Mqtt. http://mqtt.org.

[12] Opencv. http://opencv.org.

[13] Tensorflow. https://www.tensorflow.org.

[14] Wonder Shaper. http://lartc.org/wondershaper/.

[15] P. Bellavista and A. Zanni. Feasibility of fog computing deployment based on docker containerization over RaspberryPi. In *Proc. of ACM Conference on Distributed Computing and Networking (ICDCN)*, Hyderabad, India, January 2017.

[16] F. Bonomi, R. Milito, J. Zhu, and S. Addepalli. Fog computing and its role in the internet of things. In *Proc. of ACM SIGCOMM workshop on Mobile Cloud Computing (MCC)*, Helsinki, Finland, August 2012.

[17] V. Cardellini, V. Grassi, F. Lo, and M. Nardelli. Distributed QoS-aware scheduling in storm. In *Proc. of ACM International Conference on Distributed Event-Based Systems (DEBS)*, Oslo, Norway, June 2015.

[18] V. Cardellini, V. Grassi, F. Presti, and M. Nardelli. Optimal operator placement for distributed stream processing applications. In *Proc. of ACM International Conference on Distributed and Event-based Systems (DEBS)*, Irvine, CA, June 2016.

[19] R. Eidenbenz and T. Locher. Task allocation for distributed stream processing. In *Proc. of IEEE INFOCOM*, San Francisco, CA, USA, April 2016.

[20] R. Friedman, A. Kogan, and Y. Krivolapov. On power and throughput tradeoffs of WiFi and Bluetooth in smartphones. *IEEE Transactions on Mobile Computing*, 12(2):1363–1375, 2013.

[21] K. Giang, M. Blackstock, R. Lea, and C. Leung. Developing IoT applications in the fog: A distributed dataflow approach. In *Proc. of IEEE International Conference on Internet of Things (IoT)*, Seoul, South Korea, December 2015.

[22] M. Hirzel, R. Soule, S. Schneider, B. Gedik, and R. Grimm. A catalog of stream processing optimizations. *ACM transactions on Computing Surveys*, 46(4), 2014.

[23] H. Hong, J. Chuang, and C. Hsu. Animation rendering on multimedia fog computing platforms. In *Proc. of IEEE International Conference on Cloud Computing Technology and Science (CloudCom)*, Luxembourg, December 2016.

[24] Z. Khayyat, K. Awara, A. Alonazi, H. Jamjoom, D. Williams, and P. Kalnis. Mizan: a system for dynamic load balancing in large-scale graph processing. In *Proc. of ACM European Conference on Computer Systems (EuroSys)*, Prague, Czech Republic, April 2013.

[25] G. Malewicz, H. Austern, J. Bik, C. Dehnert, I. Horn, N. Leiser, and G. Czajkowski. Pregel: a system for large-scale graph processing. In *Proc. of ACM SIGMOD*, Indianapolis, Indiana, USA, June 2010.

[26] K. Mikhaylov, J. Petaejaejaervi, and T. Haenninen. Analysis of capacity and scalability of the LoRa low power wide area network technology. In *Proc. of European Wireless Conference (EW)*, Oulu, Finland, May 2016.

[27] C. Pahl, S. Helmer, L. Miori, J. Sanin, and B. Lee. A container-based edge cloud paas architecture based on Raspberry Pi clusters. In *Proc. of IEEE International Conference on Future Internet of Things and Cloud Workshops (FiCloudW)*, Vienna, Austria, August 2016.

[28] C. Pahl and B. Lee. Containers and clusters for edge cloud architectures–a technology review. In *Proc. of IEEE International Conference on Future Internet of Things and Cloud Workshops (FiCloudW)*, Rome, Italy, August 2015.

[29] P. Pietzuch, J. Ledlie, J. Shneidman, M. Roussopoulos, M. Welsh, and M. Seltzer. Network-aware operator placement for stream-processing systems. In *Proc. of IEEE International Conference on Data Engineering (ICDE)*, Atlanta, GA, USA, April 2006.

[30] D. Pizzolli, G. Cossu, D. Santoro, L. Capra, C. Dupont, D. Charalampos, F. Pellegrini, F. Antonelli, and S. Cretti. Cloud4IoT: a heterogeneous, distributed and autonomic cloud platform for the IoT. In *Proc. of IEEE International Conference on Cloud Computing Technology and Science (CloudCom)*, Luxembourg, December 2016.

[31] S. Salihoglu and W. Jennifer. GPS: A graph processing system. In *Proc. of ACM International Conference on Scientific and Statistical Database Management (SSDBM)*, Baltimore, Maryland, July 2013.

[32] E. Saurez, K. Hong, D. Lillethun, U. Ramachandran, and B. Ottenwalder. Incremental deployment and migration of geo-

distributed situation awareness applications in the fog. In *Proc. of ACM International Conference on Distributed and Event-based Systems (DEBS)*, Irvine, CA, June 2016.

[33] S. Shin, S. Seo, S. Eom, J. Jung, and H. Lee. A Pub/Sub-Based fog computing architecture for Internet-of-Vehicles. In *Proc. of IEEE International Conference on Cloud Computing Technology and Science (CloudCom)*, Luxembourg, December 2016.

[34] S. Teerapittayanon, B. McDanel, and H. Kung. Distributed deep neural networks over the cloud, the edge and end devices. In *Proc. of IEEE International Conference on Distributed Computing Systems (ICDCS)*, Atlanta, GA, USA, June 2017.

[35] D. Wu, I. Arkhipov, M. Kim, L. Talcott, C. Regan, A. McCann, and N. Venkatasubramanian. ADDSEN: adaptive data processing and dissemination for drone swarms in urban sensing. *IEEE Transactions on Computers*, 66(2):183–198, 2016.